Analytica Chimica Acta 1107 (2020) 48–54

Contents lists available at ScienceDirect

Analytica Chimica Acta

journal homepage: www.elsevier.com/locate/aca

An anchored monopodial DNA walker triggered by proximity hybridization for amplified amperometric biosensing of nucleic acid and protein

Yi Man [a, b, 1], Jinbo Liu [b, 1], Jie Wu [c], Li Yin [a], Hua Pei [a], Qiang Wu [a], Qianfeng Xia [a, *], Huangxian Ju [c, **]

[a] Key Laboratory of Tropical Translational Medicine of Ministry of Education, School of Tropical Medicine and Laboratory Medicine, Hainan Medical University, Haikou, 571199, PR China
[b] Affiliated Hospital of Southwest Medical University, Luzhou, 646000, PR China
[c] State Key Laboratory of Analytical Chemistry for Life Science, School of Chemistry and Chemical Engineering, Nanjing University, Nanjing, 210023, PR China

HIGHLIGHTS

- An electrochemical biosensor amplified with anchored monopodial DNA walker and target-induced proximity hybridization is developed.
- The anchored "cleat" enlarges the surface walking steps and thus improves greatly the efficiency of signal amplification.
- The one-step and enzyme-free detection can be conveniently performed in room temperature.
- The excellent performance demonstrates the good extendability of this strategy for different targets.

GRAPHICAL ABSTRACT

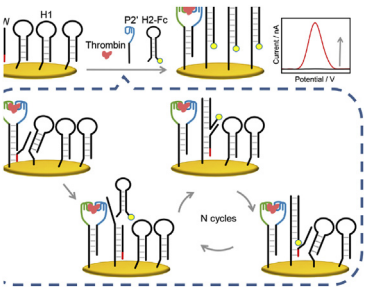

ARTICLE INFO

Article history:
Received 12 January 2020
Received in revised form
4 February 2020
Accepted 6 February 2020
Available online 7 February 2020

Keywords:
Electrochemical sensor
DNA walker
Signal amplification
Proximity hybridization
Thrombin
Nucleic acid

ABSTRACT

This work designed an anchored monopodial DNA walker to amplify amperometric biosensing signal for sensitive detection of nucleic acid and protein. The biosensing surface was constructed by self-assembling hairpin DNA1 (H1) and small amount of P1-W (probe DNA1 hybridized with walking DNA) on a gold electrode. In the presence of target molecule, the walker could be triggered by the surface proximity hybridization product of P1, target and P2 to induce the cyclic hybridization of H1 with ferrocene modified hairpin DNA2 (H2-Fc), which took electroactive Fc to the electrode surface for amplified amperometric detection of the target. By linking P1 and P2 with dual specific DNA strands, aptamers or antibodies to recognize the target for proximity hybridization of P1 and P2, the walker amplified amperometric strategy could be used for highly sensitive biosensing of different targets. Using DNA and thrombin as the target models, the proposed biosensing methods achieved the linear range from 0.2 pM to 2 nM with a detection limit of 0.11 pM and 1.0 pM to 10 nM with a detection limit of 0.61

* Corresponding author.
** Corresponding author.
E-mail addresses: xiaqianfeng@sina.com (Q. Xia), hxju@nju.edu.cn (H. Ju).
[1] Y.M. and J.B.L. contributed equally to this work.

https://doi.org/10.1016/j.aca.2020.02.013

pM, respectively. The specific recognition process endowed the strategy with high selectivity and potential applications.

1. Introduction

Enlightened by native motor protein, various artificial molecular machines, such as computer [1], walker [2], tweezer [3], robot [4] and rotor [5], have been proposed for different purposes. Given the characteristics of highly ordered and easy to design, DNA walker has attracted widespread attention especially in bioimaging [6,7] and biosensing fields [8–16] and greatly improved the sensitivity of biosensors [17–20]. As one of commonly developed DNA walkers, swing-arm walker [21] has been designed in different forms of assembly for electrochemical biosensing. For example, a "signal off" electrochemical biosensor has been achieved by using aptamer sequence to block the swing-arm, and target to trigger the walker in the presence of nicking endonuclease [22] and a swing-arm strand has been constructed by the recognition of immobilized DNA-antigen to antibody and then another DNA′-antigen for "signal on" electrochemical biosensing through cyclic proximity hybridization, ferrocene (Fc) labeled primer annealing and DNA polymerization induced walker release [23]. Obviously, these swing-arm walkers can only walk within the radius of arm strand. In order to enlarge the walking distance, some single or multiple leg walkers have been developed for one-to-all walking [24]. Unfortunately, both the triggering and the walking of above walkers needs nicking endonuclease or polymerase, which leads to the dependence of walking step on the enzyme activity and indirectly influences the walking region. Thus, a bipedal DNA walker propelled by locked nucleic acid modified toehold mediate strand displacement reaction has been proposed for electrochemical detection of microRNA [25]. Although this enzyme-free strategy uses a two-leg system to make it persist on DNA tracks, it is possible to detach walker into solution when both two legs are replaced at the same time, which also limits the walking steps and thus the amplification efficiency.

To achieve more walking steps, Ellington et al. designed a simple single-legged DNA walker with an optimized "cleat" to hold it on a particle-bound substrate and demonstrated its ability easier to be integrated into analytical detection schemes than previous double legged walkers [26]. Inspired by the "cleat" strategy, this work designed an anchored monopodial walker that was triggered with a proximity hybridization to achieve target-induced switch for amplified electrochemical biosensing.

The proximity hybridization is generally achieved by the simultaneous recognition of target molecule to two DNA-conjugated affinity ligands [27–29]. By using the proximity hybridization product to open the self-reporting molecular beacon, a series of chemiluminescent [30] or electrochemical [31–33] proximity assay methods have been developed for specific detection of target DNA or proteins. To improve the detection sensitivity, these proximity assay strategies have further been coupled with nicking endonuclease induced recycling [30] and hybridization chain reaction [34] for signal amplification.

In this work, the designed monopodial walker (W) was firstly cleated on an affinity ligand conjugated DNA strand (P1), which was then assembled on gold electrode along with a large number of hairpin DNA1 (H1) (Scheme 1). Upon the target-induced proximity hybridization of immobilized P1 and P2 in solution, the walking DNA strand was replaced by P2 from its 5′ end to open immobilized H1, the anchored "cleat" at its 3′ end was then dehybridized to bind the 5′ end of the opened H1. The 3' end of the opened H1 could recognize the ferrocene modified hairpin DNA2 (H2-Fc), which took electroactive Fc to the electrode surface and replaced the walking DNA strand for subsequent recognition and anchored walking. Theoretically, the walking DNA strand could traverse the whole biosensing surface via the continuous strand displacement reaction, which brought H2-Fc to immobilized H1 and greatly amplified the readout signal, thus leading to a robust amperometric biosensing strategy for sensitive detection of target. Using DNA and thrombin as the target models, the corresponding affinity ligands (dual specific DNA strands and aptamers) could be linked to P1 and P2 for design of two biosensing methods. The excellent performance of the proposed methods demonstrated the extendability of the monopodial DNA walker and its promising application in biosensing of nucleic acids and proteins.

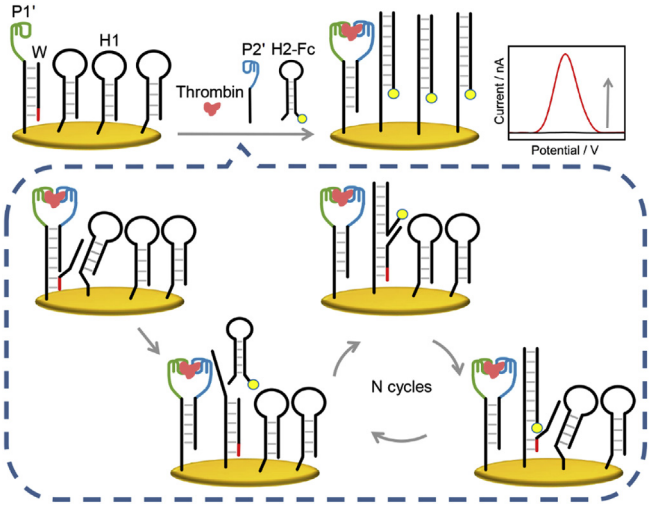

Scheme 1. Schematic illustration of the designed walker triggered by surface proximity hybridization product for amplified amperometric biosensing of protein.

2. Experimental

2.1. Materials and reagents

Anthropogenic thrombin, tris (2-carboxyethyl) phosphine hydrochloride (TCEP), mercaptohexanol (MCH) and N, N, N′, N′-tetramethylethylenediamine (TEMED) were purchased from Sigma-Aldrich (St. Louis, MO, USA). Carcinoembryonic antigen (CEA) and α-fetoprotein (AFP) were purchased from Keybiotech Co. Ltd. (Beijing, China). Ultrapure water was obtained from Millipore water purification system (≥18MΩ, Milli-Q, Millipore) and used throughout the experiment. Tris-HCl buffer (30 mM, pH 7.4) contained 140 mM NaCl, 5 mM KCl, 1 mM $MgCl_2$ and 1 mM $CaCl_2$. PBS buffer (10 mM, pH 7.4) contained 137 mM NaCl. The serum samples were from Jiangsu Cancer Hospital and stored at −20 °C before use. O'RangeRuler 20bp DNA ladder, 6 × DNA loading buffer and 10000x SYBR Gold dye was purchased from Bio-Rad Co. Ltd (Hercules,

California, USA). 20 × PBS which was diluted to 1 × as washing buffer, premixed 10 × TBE powder, 30% methylene acrylamide and all oligonucleotides were obtained from Sangon Biotech Co. Ltd. (Shanghai, China). The oligonucleotides were purified by high performance liquid chromatography, and their sequences were listed as follows:

P1:

5′-SH-$(CH2)_6$-GCCATTTCGTCAGTGAGC*TAGGTTA-GATGTCG*TTTTTTTTTT-TTTTTTTTTT**CACCGTATGCTACTGTAGAT**-3′

P2: 5′-**TAGGAAAAGGAGGAGGGTGG**TTTTTTTTTTTTTTTTTTTTC-*GACATC-TAACCTA*-3′

W(0B):

5′-CGACATCTAACCTAGCTCACTGAC-3′

W(2B):

5′-CGACATCTAACCTAGCTCACTGACGA-3′

W(4B):

5′-CGACATCTAACCTAGCTCACTGACGAAA-3′

W(6B):

5′-CGACATCTAACCTAGCTCACTGACGAAATG-3′

W(8B):

5′-CGACATCTAACCTAGCTCACTGACGAAATGGC-3′

H1:

5′-SH-(CH2)6-GCCATTTCGTCAGTGAGCTAGGTTA-GATGTCGCCATGTGTA-GACGACATCTAACCTAGC-3′

H2-Fc:

5′-AGATGTCGTCTACACATGGCGA-CATCTAACCTAGCCCATGTGTAGA-CTCACTGAC-Ferrocene-3′

Target DNA:

5′-CCACCCTCCTCCTTTTCCTATTTTCTTTAATTTCTTATTTCTCTT-AA TTTTAATTTGTTTATCTACAGTAGCATACGGTG-3′

P1':

5′-HS-$(CH2)_6$-GCCATTTCGTCAGTGAGC*TAGGTTA-GATGTCG*TTTTTTTTTT-TTTTTTTTTT**GGTTGGTGTGGTTGG**-3′

P1'':

5′-GCCATTTCGTCAGTGAGC*TAGGTTA-GATGTCG*TTTTTTTTTTTTTTTTT-TTT**GGTTGGTGTGGTTGG**-3′

P2':

5′-**AGTCCGTGGTAGGGCAGGTTGGGGT-GACT**TTTTTTTTTTTTTTTTT-TT*CGACATCTAACCTA*-3′

The complementary sequences of P1 with P2, P1′ or P1″ with P2′ are shown in italic, the sequences of "cleat" in W and the complementary sequence in H1 are shown in underline, the specific DNA strands and aptamer sequences for recognition of target DNA and thrombin in P1, P2, P1′ and P2', are shown in bold, respectively.

2.2. Apparatus

Electrochemical electrode arrays were composed of 16 sensors, which were from Ninghaijieyi Biotech LLC (Ningbo, China). Each sensor contained a gold working electrode (3 mm in diameter), a gold auxiliary electrode and a gold reference electrode. The electrode arrays were prepared by electronic beam evaporation for single use, and thus could not be treated through Piranha solution immersion. Differential pulse voltammetric (DPV) measurements were performed on a CHI 1040C electrochemical workstation (CH Instruments Inc., Austin, USA) at room temperature. Electrochemical impedance spectroscopic (EIS) measurements were performed on VersaSTAT 3 electrochemical analyzer (Princeton Applied Research, USA) with external platinum wire counter electrode and Ag/AgCl reference electrode. Gel electrophoresis analysis was performed using Bio-Rad ChemDoc XRS (Bio-Rad, USA).

2.3. Fabrication of electrochemical biosensor

P1-W was firstly formed by mixing 20 μM P1 and 20 μM W at 1:1 (*V*/*V*) to denature at 95 °C for 5 min and then slowly cooling down to room temperature. After 3 μl of the mixture of H1 (1 μM), P1-W (0.03 μM), and TCEP (1 mM) was incubated at 37 °C for 1 h to reduce disulfide bonds, it was dropped on newly gold electrode to incubate at 37 °C for 2 h. Afterward the electrode was rinsed with 10 mM PBS (pH 7.4, 0.1 M NaCl) and dried with nitrogen, and 3 μl of 1 mM MCH was dropped on its surface to block the unmodified sites. After washed with 10 mM PBS and dried with nitrogen, the electrochemical biosensor was obtained for DNA detection. The biosensor for thrombin was fabricated with P1' in a similar procedure.

2.4. Detection of target DNA and thrombin

Prior to measurement, various concentrations of target DNA were firstly mixed with 2 μM H2-Fc and 100 nM P2 in 10 mM PBS for at least 15 min. 3 μl of the mixture was then dropped on above DNA biosensor surface to incubate for 90 min at room temperature. After the biosensor was washed with 10 mM PBS and dried with nitrogen, 40 μl of 10 mM PBS containing 100 mM $NaClO_4$ was dropped on three-electrode region to perform the DPV measurement from −0.05 V to +0.35 V (vs. Au reference electrode) with an increment potential of 0.004 V, an amplitude potential of 0.05 V, and a pulse width of 0.5 s.

Similarly, the detection of thrombin was performed with P1′-W and H1 co-modified electrode by mixing 2 μM H2-Fc, 100 nM P2′ and various concentrations of thrombin in Tris-HCl (30 mM, pH 7.4) [35,36].

2.5. Polyacrylamide gel electrophoresis (PAGE)

Non-denatured hydrogel was prepared using 12% gel solution. The electrophoresis was carried out at 100 V, 90 min, and in 1 × TBE with external ice bath to reduce the gel thermal deformation. The gel was stained using SYBR Gold dye and placed in dark for 30 min, and photographed under UV irradiation.

3. Results and discussion

3.1. Principle of electrochemical biosensing

H1 and P1-W (or P1′-W) at a ratio of 100:3 were self-assembled on gold electrode surface through Au-S bond. P1 or P1′ contained 3 regions: specific DNA strand for DNA or aptamer for thrombin (ID# 64 in aptamer database Aptagen) as affinity ligand at 3′ end, poly T spacer sequence to reduce the steric hindrance, and a sequence complementary with W. In the reaction solution, P2 or P2′ contained another specific DNA strand for DNA or aptamer (ID# 315 in aptamer database Aptagen) for thrombin at 5′ end, poly T spacer and a sequence complementary with to 5′ end of P1 or P1'. The W was complementary with the 5′ end of H1, at which H1 was immobilized on the electrode surface, and H2-Fc was complementary with H1 from the 3′ end. In the absence of target, the binding between P1 and P2 could not happen due to the thermodynamic stability. As shown in Scheme 1, after the mixture containing target, P2 or P2′, and H2-Fc was added to the biosensor surface, the proximity hybridization among P1 or P1′, target DNA or protein, P2 or P2′ respectively resulted in a strand displacement reaction to release the 5′ end of W, which hybridized with neighboring H1 and then completely peeled from P1 or P1′ to bind onto the 5′ end of H1. Upon the recognition of the opened H1 to H2, another strand displacement reaction induced the release of the 5′ end of W from the H1 strand and the introduction of electroactive Fc group labeled at the 3′ end of H2 onto electrode surface. The released 5′ end of W subsequently hybridized with another neighboring H1 before the complete separation of the “cleat” from foregoing H1. In the end, a plenty of H2-Fc were bound to the immobilized H1 to generate significant current signal for amplified amperometric biosensing.

3.2. Feasibility characterization

The feasibility of continuous strand displacement reaction for cleated DNA walking was characterized via PAGE analysis. The mixture of H1 and H2 showed two clear bands of H1 and H2 respectively, and no new band was observed (Fig. 1A, lanes 2–4), indicating the absence of the direct hybridization. Here lane 2 showed a weak layer, which possibly resulted from the conformation change at the tail of H1 (Fig. S1). After W was mixed with H1, both bands of H1 and W disappeared, and a new band occurred at greater weight (Fig. 1A, lanes 1, 2 and 5), indicating the hybridization of H1 and W to form H1-W. When W was mixed with H1 and H2 at the same amount, the hybridization complex of H1, W and H2 (H1-W-H2) could be formed at greater weight, while H1-H2, H1-W, and left H2 could also be observed (Fig. 1A, lane 7), demonstrating the presence of W-triggered strand displacement reaction for the formation of H1-H2.

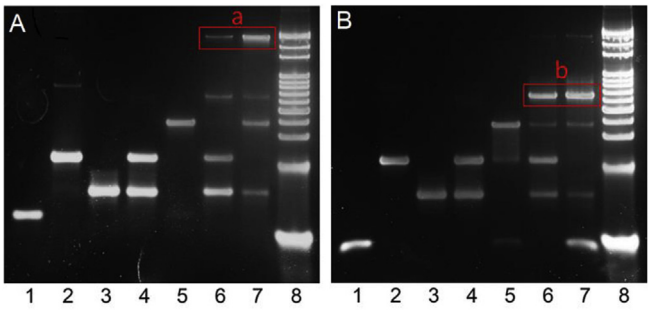

Fig. 1. PAGE analysis of walker feasibility: (A) lane 1, W(6B); lane 2, H1; lane 3, H2; lane 4, mixture of H1 and H2; lane 5, mixture of H1 and W(6B); lane 6, mixture of H1 and H2 containing 10% W(6B); lane 7, mixture of H1, H2 and W(6B) at 1:1:1; lane 8, DNA marker; and (B) lane 1, W(0B); lane 2, H1; lane 3, H2; lane 4, mixture of H1 and H2; lane 5, mixture of H1 and W(0B); lane 6, mixture of H1 and H2 containing 10% W(0B); lane 7, mixture of H1, H2 and W(0B) at 1:1:1; lane 8, DNA marker.

Interestingly, after a small amount of W was added in the mixture H1 and H2, the band of W did not occur, while the bands for H1 and H2 weakened, and two new bands attributed to H1-H2 and H1-W-H2 occurred, respectively (Fig. 1A, lane 6). The difference in the band brightness indicated the less amount of H1-W-H2 than that of H1-H2. Thus the presence of W induced the formation of more H1-H2 via the continuous strand displacement reaction. More importantly, when using W(0B) to replace W(6B), the mixture of W(0B), H1 and H2 did not show the band of H1-W-H2, and more H1-H2 than the mixture of W(6B), H1 and H2 could be formed (Fig. 1B, square b), indicating the “cleat” with 6 bases could anchor the W on both H1 and the complex of H1-H2 for anchored walking on the electrode surface.

3.3. Characterization for biosensing fabrication and recognition

Using W(6B) as the optimized W strand, the fabrication process of the biosensor and its recognition to target molecule were characterized with EIS measurements in 0.1 M KCl containing 5 mM $K_3Fe(CN)_6/K_4Fe(CN)_6$ from 0.1 to 10,000 Hz with an amplitude of 0.01 V and DPV detection in 10 mM PBS containing 100 mM $NaClO_4$. As shown in Fig. 2A, the bare electrode exhibited a relatively low electron transfer resistance (*R*et) (curve a), while the *R*et obviously increased after the electrode was incubated in the mixture of P1′-W and H1 (curve b), indicating the successful assembly of P1′-W and H1 on electrode surface, which led to the repelling between negatively charged phosphate skeleton and $[Fe(CN)_6]^{3-/4-}$. The blocking with MCH led to great increase of the *R*et (curve c). After the DNA walker-based thrombin biosensor was incubated with the mixture of P2′, H2-Fc and thrombin, the *R*et further increased from about 40 kΩ to 147 kΩ (curve d), indicating the immobilization of protein on the biosensor surface. The occurrence of great oxidation peak current (in this work, all mentioned “peak current” means peak value of current) in the DPV curve (Fig. 2B, curve d) demonstrated the introduction of electroactive Fc group through the walking DNA-induced strand displacement reaction. It should be pointed out that the electrode arrays was prepared by electron beam evaporation to deposit a thick gold layer (about 50 nm), thus the bare electrode showed higher impedance than general gold electrode. The much weaker DPV response of the biosensor incubated with 30 mM Tris-HCl containing 2 μM H2-Fc (curve b) or 2 μM H2-Fc + 100 nM P2' (curve c) than that in the presence of 100 pM thrombin (curve d) could be attributed the adsorption of a little H2-Fc, which could be treated as the background.

3.4. Optimization for thrombin detection

To obtain the efficient performance of the biosensor for thrombin detection, the concentration of H1 and the ratio of P1′-W to H1 for biosensor fabrication, the concentration of H2-Fc and the reaction time were optimized. The biosensing response obviously depended on both the amount and the surface density of H1 for binding of H2-Fc. With the increasing H1 concentration, the amount of assembled H1 increased, thus the DPV peak current of bound H2-Fc increased (Fig. 2C). However, high loading of H1 was detrimental to the binding of H2-Fc due to the steric hindrance, which led to the decrease of the peak current. The optimal concentration of H1 was 1.0 μM, at which the concentration ratio of P1′-W to H1 biosensor preparation was optimized to be 1:30 (Fig. 2D). It means that a little target could take a large number of

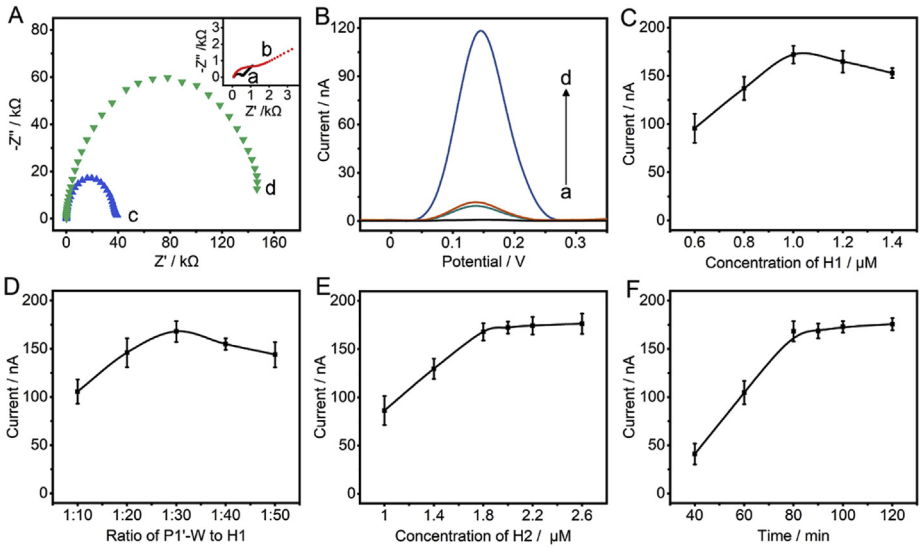

Fig. 2. (A) EIS Nyquist plots of (a) bare and (b) P1′-W/H1 modified electrodes, (c) MCH blocked (b), and (d) (c) after incubation with 30 mM Tris-HCl containing 100 pM thrombin, 100 nM P2′ and 2 μM H2-Fc. (B) DPV curves of the biosensor after incubation with (a) 30 mM Tris-HCl, (b) (a) + 2 μM H2-Fc, (c) (b) + 100 nM P2′, and (d) (c) + 100 pM thrombin. Optimization of (C) H1 concentration and (D) ratio of P1′-W to H1 for biosensor preparation, and (E) H2-Fc concentration and (F) incubation time for thrombin detection. Error bars represent standard deviations of three parallel experiments.

H2-Fc to biosensor surface through the target-induced proximity hybridization and then DNA walking triggered continuous strand displacement reaction, which greatly amplified the amperometric response for thrombin detection.

The concentration of H2-Fc used for strand displacement reaction and the reaction time were optimized to be 2.0 μM and 90 min, respectively (Fig. 2E and F). At higher H2-Fc concentration and longer reaction time, the DPV peak current trended to the maximum value, indicating the saturated binding of H2-Fc to the immobilized H1.

3.5. Detection performance of biosensor for thrombin

Under optimal conditions, the DPV peak current increased with the increasing thrombin concentration from 0.1 pM to 20 nM (Fig. 3A). The plot of peak current vs the logarithm of thrombin concentration showed very good linearity in the concentration range of 1.0 pM–10 nM, following the regression equation of $I = 51.73 \text{ Log } C + 26.51$ with a correlation coefficient of 0.9975 (Fig. 3B). The limit of detection was calculated to be 0.61 pM at 3 times standard deviation of background, which was 4 fold lower than that of swing-arm walker based strategy [37], and much lower than those of DNA-based electrochemical methods [38–41], as listed in Table S1. It was worth mentioning that, the reaction time was optimized at 1.0 nM thrombin, the limit of detection could be further decreased at longer reaction time.

The biosensing specificity was evaluated using AFP and CEA at the concentration 10 times that of thrombin (Fig. 3C). In contrast of blank, both AFP and CEA did not show obvious signal, and the mixture of thrombin with AFP and CEA showed significant response with the same peak current as that for thrombin, indicating the excellent specificity of the biosensor and that the coexisting proteins did not interfere with the detection of thrombin.

To figure out the advantages of the designed strategy, a biosensing method by using the proximity hybridization product of P1″-W, thrombin and P2′ in solution to trigger the walking for continuous strand displacement reaction (Fig. S2A). Here P1″ possesses the same sequence as P1′, and the biosensor was prepared by dropping 3 μl mixture of H1 (1 μM) and TCEP (1 mM) on gold electrode to incubate at 37 °C for 2 h. For thrombin detection, a mixture containing 2 μM H2-Fc, 100 nM P2′, 0.03 μM P1″-W and different concentrations of thrombin were dropped on the biosensor surface to incubate for 90 min at room temperature. The plot of DPV peak current vs the logarithm of thrombin concentration showed the linearity in 10 pM to 10 nM (Fig. S2B). The relatively lower sensitivity than that based on the surface proximity

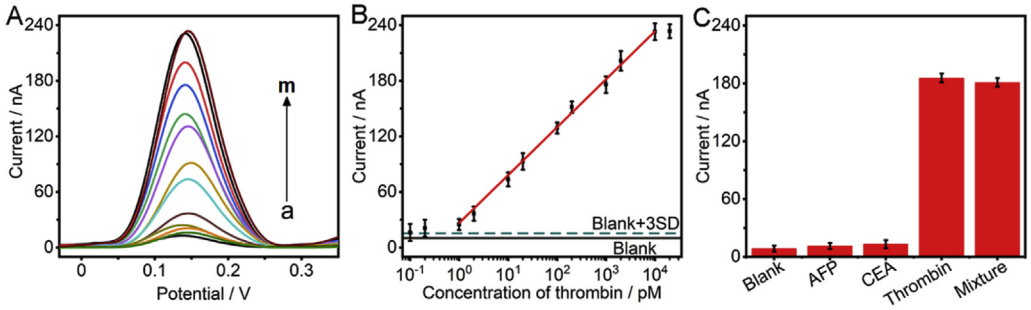

Fig. 3. (A) DPV curves of the biosensor for 0, 0.1, 0.2, 1.0, 2.0, 10, 20, 100 and 200 pM (a-i), and 1.0, 2.0, 10 and 20 nM (j-m) thrombin. (B) Plot of peak current vs logarithm of thrombin concentration. (C) Responses of biosensor for detection of 10 nM AFP, 10 nM CEA, 1.0 nM thrombin and the mixture of 10 nM AFP, 10 nM CEA and 1.0 nM thrombin. Error bars represented standard deviations of three parallel experiments.

Table 1
Recovery for detection of thrombin in diluted serum samples.

Sample no.	Added/pM	Found/pM	Recovery/%	RSD [a]/%
1	10	9.792	97.9	6.49
2	20	19.47	97.4	6.20
3	100	98.48	98.5	4.78
4	200	204.3	102.2	4.36
5	1000	1008	100.8	4.51

[a] The mean of three measurements.

hybridization triggered DNA walking indicated that the triggering of DNA walking by proximity hybridization product formed in solution was more difficult. Thus this strategy was better than multi-leg strategy in the same conditions due to the long dwell time of W resulted from the "cleat".

The detection accuracy of the biosensing strategy was examined by performing recovery test of thrombin in 10-fold diluted clinical human serum sample from Jiangsu Cancer Hospital. As shown in Table 1, the recovery of thrombin was from 97.4% to 102.2% in the concentration range of 10 pM to 1.0 nM, and the RSDs for three measurements were from 4.36% to 6.49%, indicating the good accuracy and acceptable precision.

3.6. Detection of target DNA

To achieve the detection of target DNA with the designed monopodial walker, two specific DNA strands for target DNA were bound at 3′ end of P1 and 5' end of P2. After the mixture of target DNA with P2 and H2-Fc was dropped on corresponding biosensor to incubate at room temperature for 90 min (Fig. 4A), the DPV signal was detected for optimizing the conditions of biosensor fabrication and DNA analysis. When 0.03 μM P1-W was used for preparation of the biosensor, the DPV response increased with the increasing H1 concentration, and reached the maximum value at 1.0 μM (Fig. 4B), at which the suitable ratio of P1-W to H1 was also 1:30 (Fig. 4C). Thus the mixture of 0.03 μM P1-W and 1.0 μM H1 was used for co-immobilization of P1-W and H1.

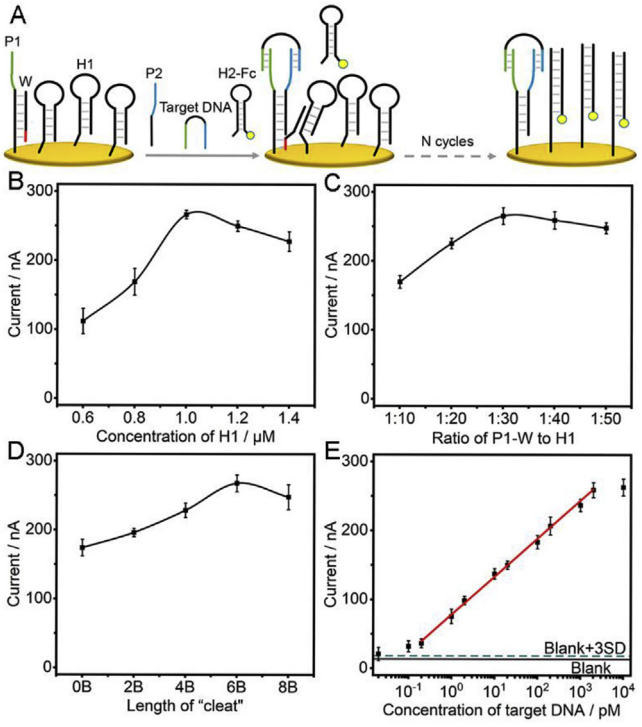

Fig. 4. (A) Schematic illustration of the walker triggered by using DNA as target. Optimization of (B) H1 concentration, (C) ratio of P1-W to H1, and (D) length of "cleat" for DNA detection. (E) Plot of peak current vs logarithm of DNA concentration. Error bars represent standard deviations of three parallel experiments.

The anchored walking depended on the length of designed "cleat" at 3' end of W, while the length of toehold did not significantly influence the efficiency of toehold mediated strand displacement reaction when it was longer than 8 nt [42]. Thus we examined the effect of "cleat" length on the response with the toehold length beyond 8 nt. The short "cleat" made it difficult to anchor the walker on biosensor surface, which led to the leakage of the waking DNA strand from the surface and thus decreased the walking efficiency. However the too long "cleat" endowed the double stranded P1-cleat and cleat-H1 with better stability, which decreased the walking rate and thus the amplification efficiency. The maximum response occurred at the "cleat" length of 6 nt (Fig. 4D). Therefore, W(6B) was chosen as the optimal walking strand.

Similarly, the DPV peak current increased with the increasing target DNA concentration under optimal conditions. The plot of peak current vs the logarithm of DNA concentration followed the equation $I = 55.22 \text{ Log } C + 78.13$ in the concentration range of 0.2 pM–2.0 nM with a correlation coefficient of 0.9987 (Fig. 4E). The detection limit was calculated to be 0.11 pM at 3 times standard deviation of background. The analytical performance was comparable with those of DNA-amplified electrochemical methods (Table S2), indicating its application potential.

4. Conclusion

This work designs an anchored monopodial walker to perform the "one-to-all" walking amplification strategy. By self-assembling a little P1-W and a large number of H1 on gold electrode surface, the DNA walking based electrochemical biosensor can be conveniently prepared. The DNA walker can be triggered with a target-induced surface proximity hybridization, which causes continuous strand displacement reaction to take the electroactive H2-Fc to biosensor surface for amplified amperometric biosensing. Different from swing-arm or multi-leg walkers, this strategy conducts an optimal "cleat" as the anchor sequence to prolong the dwelling time of walker on biosensor surface and increase the walking efficiency. Using DNA and thrombin as the target models, this work uses dual specific DNA strands and aptamers to demonstrate the excellent performance and extendability of the designed strategy for detection of DNA and proteins. Therefore, the proposed one-step and enzyme-free biosensing strategy possesses promising application in analysis of proteins and nucleic acids.

Declaration of competing interest

The authors declare that they have no known competing financial interests or personal relationships that could have appeared to influence the work reported in this paper.

CRediT authorship contribution statement

Yi Man: Conceptualization, Data curation, Investigation, Methodology, Writing - original draft. **Jinbo Liu:** Conceptualization, Methodology, Supervision, Writing - original draft. **Jie Wu:** Data curation, Investigation. **Li Yin:** Data curation, Investigation. **Hua Pei:** Data curation, Investigation. **Qiang Wu:** Data curation, Investigation. **Qianfeng Xia:** Conceptualization, Methodology, Supervision, Funding acquisition, Resources, Writing - original draft. **Huangxian Ju:** Writing - original draft, Conceptualization, Methodology, Supervision, Funding acquisition, Resources, Writing -

review & editing.

Acknowledgements

This work was financially supported by National Science and Technology Major Project (No. 2018ZX10101003-001009) and the National Natural Science Foundation of China (21635005, 21827812, 21890741).

Appendix A. Supplementary data

Supplementary data to this article can be found online at https://doi.org/10.1016/j.aca.2020.02.013.

References

[1] Y. Benenson, B. Gil, U. Ben-Dor, R. Adar, E. Shapiro, An autonomous molecular computer for logical control of gene expression, Nature 429 (2004) 423–429.
[2] J.S. Shin, N.A. Pierce, A synthetic DNA walker for molecular transport, J. Am. Chem. Soc. 126 (2004) 10834–10835.
[3] M. Liu, J. Fu, C. Hejesen, Y. Yang, N.W. Woodbury, K. Gothelf, Y. Liu, H. Yan, A DNA tweezer-actuated enzyme nanoreactor, Nat. Commun. 4 (2013) 1–5.
[4] A.J. Thubagere, W. Li, R.F. Johnson, Z. Chen, S. Doroudi, Y.L. Lee, G. Izatt, S. Wittman, N. Srinivas, D. Woods, E. Winfree, L. Qian, A cargo-sorting DNA robot, Science 357 (2017), eaan6558.
[5] J. Valero, N. Pal, S. Dhakal, N.G. Walter, M. Famulok, A bio-hybrid DNA rotor-stator nanoengine that moves along predefined tracks, Nat. Nanotechnol. 13 (2018) 496–503.
[6] C.P. Liang, P.Q. Ma, H. Liu, X. Guo, B.C. Yin, B.C. Ye, Rational engineering of a dynamic, entropy-driven DNA nanomachine for intracellular microRNA imaging, Angew. Chem. Int. Ed. 56 (2017) 9077–9081.
[7] M. Xu, J. Zhuang, X. Jiang, X. Liu, D. Tang, A three-dimensional DNA walker amplified FRET sensor for detection of telomerase activity based on the MnO2 nanosheet-upconversion nanoparticle sensing platform, Chem. Commun. 55 (2019) 9857–9860.
[8] J. Zhuang, W. Lai, G. Chen, D. Tang, A rolling circle amplification-based DNA machine for miRNA screening coupling catalytic hairpin assembly with DNAzyme formation, Chem. Commun. 50 (2014) 2935–2938.
[9] X. Qu, D. Zhu, G. Yao, S. Su, J. Chao, H. Liu, X. Zuo, L. Wang, J. Shi, L. Wang, W. Huang, H. Pei, C. Fan, An exonuclease III-powered, on-particle stochastic DNA walker, Angew. Chem. Int. Ed. 56 (2017) 1855–1858.
[10] N. Li, J. Zheng, C. Li, X. Wang, X. Ji, Z. He, An enzyme-free DNA walker that moves on the surface of functionalized magnetic microparticles and its biosensing analysis, Chem. Commun. 53 (2017) 8486–8488.
[11] X. Zhang, Z. Yang, Y. Chang, M. Qing, R. Yuan, Y. Chai, Novel 2D-DNA-nanoprobe-mediated enzyme-free-target-recycling amplification for the ultrasensitive electrochemical detection of microRNA, Anal. Chem. 90 (2018) 9538–9544.
[12] J. Zhu, H. Gan, J. Wu, H. Ju, Molecular machine powered surface programmatic chain reaction for highly sensitive electrochemical detection of protein, Anal. Chem. 90 (2018) 5503–5508.
[13] S. Lv, K. Zhang, Y. Zeng, D. Tang, Double photosystems-based 'Z-scheme' photoeletrochemical sensing mode for ultrasensitive detection of disease biomarker accompanying 3D DNA walker, Anal. Chem. 90 (2018) 7086–7093.
[14] J. Wang, D. Wang, A. Tang, D. Kong, Highly integrated, biostable, and self-powered DNA motor enabling autonomous operation in living bodies, Anal. Chem. 91 (2019) 5244–5251.
[15] S. Lv, K. Zhang, L. Zhu, D. Tang, ZIF-8 assisted NaYF4:Yb,Tm@ZnO converter with exonuclease III-powered DNA walker for near-infrared light responsive biosensor, Anal. Chem. 92 (2020) 1470–1476.
[16] J. Wang, D. Wang, A. Tang, D. Kong, Recent advances in photoelectrochemical sensing: from engineered photoactive materials to sensing devices and detection modes, Anal. Chem. 92 (2020) 363–377.
[17] Q. Zhang, F. Chen, F. Xu, Y. Zhao, C. Fan, Target-triggered three-way junction structure and polymerase/nicking enzyme synergetic isothermal quadratic DNA machine for highly specific, one-step, and rapid microRNA detection at attomolar level, Anal. Chem. 86 (2014) 8098–8105.
[18] C. Li, X. Li, L. Wei, M. Liu, Y. Chen, G. Li, Simple electrochemical sensing of attomolar proteins using fabricated complexes with enhanced surface binding avidity, Chem. Sci. 6 (2015) 4311–4317.
[19] Q. Feng, X. Zhao, Y. Guo, M. Liu, P. Wang, Stochastic DNA walker for electrochemical biosensing sensitized with gold nanocages@graphene nanoribbons, Biosens. Bioelectron. 108 (2018) 97–102.
[20] J. Liu, Z. Tang, J. Zhang, Y. Chai, Y. Zhuo, R. Yuan, Morphology-controlled 9,10-diphenylanthracene nanoblocks as electrochemiluminescence emitters for microRNA detection with one-step DNA walker amplification, Anal. Chem. 90 (2018) 5298–5305.
[21] H. Zhang, M. Lai, A. Zuehlke, H. Peng, X.F. Li, X.C. Le, Binding-induced DNA nanomachines triggered by proteins and nucleic acids, Angew. Chem. Int. Ed. 54 (2015) 14326–14330.
[22] Q. Pu, J. Li, J. Qiu, X. Yang, Y. Li, D. Yin, X. Zhang, Y. Tao, S. Sheng, G. Xie, Universal ratiometric electrochemical biosensing platform based on mesoporous platinum nanocomposite and nicking endonuclease assisted DNA walking strategy, Biosens. Bioelectron. 94 (2017) 719–727.
[23] Z. Chen, C. Wang, L. Hao, R. Gao, F. Li, S. Liu, Proximity recognition and polymerase-powered DNA walker for one-step and amplified electrochemical protein analysis, Biosens. Bioelectron. 128 (2019) 104–112.
[24] S. Cai, M. Chen, M. Liu, W. He, Z. Liu, D. Wu, Y. Xia, H. Yang, J. Chen, A signal amplification electrochemical aptasensor for the detection of breast cancer cell via free-running DNA walker, Biosens. Bioelectron. 85 (2016) 184–189.
[25] J. Zhang, L. Wang, M. Hou, Y. Xia, W. He, A. Yan, Y. Weng, L. Zeng, J. Chen, A ratiometric electrochemical biosensor for the exosomal microRNAs detection based on bipedal DNA walkers propelled by locked nucleic acid modified toehold mediate strand displacement reaction, Biosens. Bioelectron. 102 (2018) 33–40.
[26] C. Jung, P. Allen, A. Ellington, A simple, cleated DNA walker that hangs on to surfaces, ACS Nano 11 (2017) 8047–8054.
[27] S. Fredriksson, M. Gullberg, J. Jarvius, C. Olsson, K. Pietras, S.M. Gústafsdóttir, A. Östman, U. Landegren, Protein detection using proximity-dependent DNA ligation assays, Nat. Biotechnol. 20 (2002) 473–477.
[28] F. Li, H. Zhang, Z. Wang, X. Li, X.F. Li, X.C. Le, Dynamic DNA assemblies mediated by binding-induced DNA strand displacement, J. Am. Chem. Soc. 135 (2013) 2443–2446.
[29] F. Li, Y. Tang, S.M. Traynor, X.F. Li, X.C. Le, Kinetics of proximity-induced intramolecular DNA strand displacement, Anal. Chem. 88 (2016) 8152–8157.
[30] C. Zong, J. Wu, M. Liu, L. Yang, L. Liu, F. Yan, H. Ju, Proximity hybridization-triggered signal switch for homogeneous chemiluminescent bioanalysis, Anal. Chem. 86 (2014) 5573–5578.
[31] K. Ren, J. Wu, F. Yan, H. Ju, Ratiometric electrochemical proximity assay for sensitive one-step protein detection, Sci. Rep. 4 (2014) 1–6.
[32] K. Ren, J. Wu, F. Yan, Y. Zhang, H. Ju, Immunoreaction-triggered DNA assembly for one-step sensitive ratiometric electrochemical biosensing of protein biomarker, Biosens. Bioelectron. 66 (2015) 345–349.
[33] F. Zhou, Y. Yao, J. Luo, X. Zhang, Y. Zhang, D. Yin, F. Gao, P. Wang, Proximity hybridization-regulated catalytic DNA hairpin assembly for electrochemical immunoassay based on in situ DNA template-synthesized Pd nanoparticles, Anal. Chim. Acta 969 (2017) 8–17.
[34] Q. Xiao, J. Wu, P. Dang, H. Ju, Multiplexed chemiluminescence imaging assay of protein biomarkers using DNA microarray with proximity binding-induced hybridization chain reaction amplification, Anal. Chim. Acta 1032 (2018) 130–137.
[35] C. Louis, L.C. Bock, L.C. Griffin, J.A. Latham, E.H. Vermaas, Toole, Selection of single-stranded DNA molecules that bind and inhibit human thrombin, Nature 355 (1992) 564–566.
[36] D.M. Tasset, M.F. Kubik, W. Steiner, Oligonucleotide inhibitors of human thrombin that bind distinct epitopes, J. Mol. Biol. 272 (1997) 688–698.
[37] Y. Ji, L. Zhang, L. Zhu, J. Lei, J. Wu, H. Ju, Binding-induced DNA walker for signal amplification in highly selective electrochemical detection of protein, Biosens. Bioelectron. 96 (2017) 201–205.
[38] J. Yang, B. Dou, R. Yuan, Y. Xiang, Proximity binding and metal ion-dependent DNAzyme cyclic amplification-integrated aptasensor for label-free and sensitive electrochemical detection of thrombin, Anal. Chem. 88 (2016) 8218–8223.
[39] B. Jiang, F. Li, C. Yang, J. Xie, Y. Xiang, R. Yuan, Target-induced catalytic hairpin assembly formation of functional Y-junction DNA structures for label-free and sensitive electrochemical detection of human serum proteins, Sensor. Actuator. B Chem. 244 (2017) 61–66.
[40] M. Zhao, S. Zhang, Z. Chen, C. Zhao, L. Wang, S. Liu, Allosteric kissing complex-based electrochemical biosensor for sensitive, regenerative and versatile detection of proteins, Biosens. Bioelectron. 105 (2018) 42–48.
[41] J. Yang, Y. Wu, C. Gan, R. Yuan, Y. Xiang, Target-programmed and autonomous proximity binding aptasensor for amplified electronic detection of thrombin, Biosens. Bioelectron. 117 (2018) 743–747.
[42] D.Y. Zhang, G. Seelig, Dynamic DNA nanotechnology using strand displacement reactions, Nat. Chem. 3 (2011) 103–113.